Conceptual and numerical models of solute diffusion around a HLW repository in clay

J. Samper[1], A. Naves[1], C. Lu[2], Y. Li[1], B. Fritz[3] & A. Clement[3]

[1] ETS Ingenieros de Caminos, Canales y Puertos, Universidad de La Coruña, 15071-A Coruña, Spain, *jsamper@udc.es*
[2] Lawrence Livermore National Laboratory, P.O. Box 808, L-223, Livermore, CA 94550, USA, lu25@llnl.gov
[3] Laboratoire d'Hydrologie et de Géochimie de Strasbourg, Université de Strasbourg/EOST, CNRS, 1, rue Blessig, F-67084 Strasbourg Cedex, France, bfritz@unistra.fr.

Abstract

Reactive transport models have been used to simulate solute diffusion, canister corrosion, interactions of the corrosion products with the bentonite and the long-term hydrochemical evolution of porewater composition around radioactive waste repositories. Such models usually rely on simplifications of the geometry and dimensionality of the problem. Detailed three-dimensional flow and transport models, on the other hand, are used which often oversimplify the geochemical reactions. There is a clear need to identify which simplifications and assumptions are admissible. Here we present conceptual and numerical models of radionuclide diffusion and sorption around a HLW repository in clay according to the French reference concept. Models of increasing dimensionality have been performed for: 1) 1D transport perpendicular to the axes of the disposal cells; 2) 1D axisymmetric transport around disposal cells for bounded and unbounded domains; 3) 2D transport through vertical planes; and 4) 1D vertical transport from the disposal cells into the overlying Oxfordian formation. Model results are compared for simulation times up to 10^6 years and for the following radionuclides and tracers: tritium, HTO, which is treated here as an ideal and conservative tracer, $^{36}Cl^-$ which experiences anion exclusion, $^{133}Cs^+$ which sorbs moderately and ^{238}U which shows a strong sorption capacity. Radionuclides are released into the disposal cell either at a fixed concentration or as an instantaneous unit pulse. Model results indicate that the 1D unbounded model is always acceptable for ^{238}U and is valid for $^{133}Cs^+$ for $t < 10^4$ years. It is valid for HTO and $^{36}Cl^-$ only for $t < 10^3$ years. These conclusions hold true for both release modes. Computed concentrations with the 1D parallel and the 1D axisymmetric models are significantly different. Inasmuch as solute diffusion in a radioactive waste repository is expected to show radial symmetry around the cells, the use of the axisymmetric model is strongly recommended for the long-term modeling of radionuclide migration from the repository. The 1D vertical model is valid only for

conservative radionuclides released instantaneously and leads always to large errors for all radionuclides for a constant concentration.

Keywords: solute diffusion, Callovo-Oxfordian clay, numerical model,

1. Introduction

Reactive transport models have been used to simulate solute diffusion, canister corrosion, interactions of the corrosion products with the bentonite and the long-term hydrochemical evolution of porewater composition around radioactive waste repositories in clay formations (Samper et al., 2008a; Marty et al., 2010; Lu et al., 2011). Such models usually rely on simplifications of the geometry and dimensionality of the problem. Detailed three-dimensional flow and transport models, on the other hand, generally oversimplify geochemical reactions (Pepin *et al*., 2008). Integrated performance assessment calculations usually rely on simplified models to reduce the computation time. Such simplifications, however, may lead to significant errors. Simplifications in the model geometry of a radioactive waste repository have been analyzed within the framework of European Integrated Projects such as NFPRO by Mathieu et al. (2006) and Samper et al. (2007) and PAMINA by Genty *et al.* (2009). Model results derived from 1D parallel and 1D axisymmetric geochemical models of the near field of a HLW repository in clay show that the penetration into the bentonite buffer of the high pH plume caused by the degradation of the concrete liner after 10^4 years computed with a 1D radial axisymmetric model is larger than that obtained with a 1D parallel model. Solute diffusion in a 1D axisymmetric model is faster than in a 1D parallel model because the diffusive area in radial coordinates depends on the square of the radial distance, r, while it does not depend on r for a 1D parallel model (Mathieu et al. 2006; Samper et al., 2007).

There is a clear need to study and identify the appropriate assumptions and simplifications for modelling radionuclide migration in a radioactive waste repository. Here we present conceptual and numerical models of radionuclide diffusion and sorption around a HLW repository in clay according to the French reference concept (ANDRA, 2005a, 2005b). The following models of increasing dimensionality are compared: 1) 1D transport perpendicular to the axes of the disposal cells; 2) 1D axisymmetric transport around disposal cells for bounded and unbounded domains; 3) 2D transport through vertical planes; and 4) 1D

vertical transport from the disposal cells into the overlying Oxfordian formation. The paper starts with the problem formulation. Then, the numerical model is presented. Model results are discussed later. The paper ends with the main conclusions.

2. Problem formulation

In the French reference concept for vitrified waste (type C) canisters are emplaced in horizontal cells of 70 cm of diameter and 40 m of length (Andra, 2005a; 2005b). The spacing between disposal cells is equal to 13 m. Disposal cells have a metal sleeve to enable package handling for their emplacement and possible future retrieval (Figure 1). The excavation damaged zone, *EDZ*, around the cells is deemed to be irrelevant given the small diameter of the cells. Instead of the EDZ, a micro-fissured zone of a few cm may form due to the mechanical unloading (Genty et al., 2009). Such micro-cracking is expected to close soon after cell closure.

The repository will be emplaced in the Callovo-Oxfordian (C-Ox) clay formation at a depth of 65 m below the overlying Oxfordian limestone formation.

Radionuclides are released in the disposal cells. They are free to migrate into the clay formation once the canisters fail. Our model aims at simulating radionuclide migration at that stage of the evolution of the repository when the canisters have failed. At that time, the engineered barriers and the host rock are expected to be resaturated. Simulations are performed over a million years. Given the low hydraulic conductivity of C-Ox clay which ranges from $5 \cdot 10^{-14}$ to $5 \cdot 10^{-13}$ m/s (Andra, 2005a), radionuclide transport takes place mostly by molecular diffusion.

HTO is a neutral tracer which is part of the water molecule. In our calculations HTO is assumed to be an ideal and conservative tracer which neither decays nor sorbs. ^{36}Cl is the radioactive isotope of chlorine, *Cl*, which has a half-life of $3.01 \cdot 10^5$ years. Given the long simulation time, it has been treated as stable. ^{36}Cl is present mostly as the anion Cl^- which experiences anion exclusion. Caesium, *Cs*, is a fission product that is created in the UO_2 pellets during irradiation in the reactor. Although *Cs* has many isotopes, the stable isotope ^{133}Cs is the most abundant. Dissolved Cs is usually found as Cs^+, except for large Cl^- concentrations when the

concentration of CsCl(aq) may be relevant also. Cs^+ sorption onto clay occurs mainly via cation exchange. Cs^+ sorbs rapidly and achieves equilibrium almost instantaneously (Murali and Mathur, 2002; Khan, 2003; Montavon et al., 2006; Samper et al., 2010).

The most abundant isotope of uranium is ^{238}U. Given its very long half-life ($4.47 \cdot 10^9$ years), it can be treated as a stable isotope. In a deep underground radioactive waste repository, the subsurface water has reducing properties in natural conditions. U(IV) has a very low migration ability due to the formation of the poorly soluble hydroxide $U(OH)_4$ (Duro et al., 2006; Omel'yanenko et al., 2007). The dissolved concentration of uranium in subsurface water is usually smaller than 10^{-8} mol/L due to the low solubility of U under near-neutral and reducing conditions (Duro et al., 2006; Omel'yanenko et al., 2007). U sorption occurs by cation exchange and surface complexation. The K_d of U(IV) in bentonite ranges from 3.6 10^3 to 1.113 10^6 L/Kg (Vahlund et al., 2006).

3. Numerical model

3.1 Solute transport equation

The transport equation for a radionuclide which diffuses through a low permeability medium is given by (Bear, 1972):

$$\nabla \cdot (\bar{D}_e \cdot \nabla c) = \alpha \frac{\partial c}{\partial t} \qquad (1)$$

where c [ML^{-3}] is the radionuclide concentration, t [T] is time, α [-] is the capacity factor which is given by:

$$\alpha = \phi_{acc} + \rho K_d \qquad (2)$$

where Φ_{cc} [-] is the accessible porosity which is equal to the total porosity if the radionuclide is not affected by anion exclusion, K_d [L^3M^{-1}] is the distribution coefficient, and ρ [ML^{-3}] is the bulk density. $\bar{D}_e$ [L^2T^{-1}] is the effective diffusion tensor which in a coordinate system defined along the bedding planes is given by

$$\bar{D}_e = \begin{pmatrix} D_{e//} & 0 & 0 \\ 0 & D_{e//} & 0 \\ 0 & 0 & D_{e\perp} \end{pmatrix} \qquad (3)$$

where $D_{e//}$ and $D_{e\perp}$ are the components of the tensor parallel and normal to the bedding, respectively.

The apparent diffusion coefficient, D_a, takes into account the combined effect of diffusion and sorption and is defined as

$$D_a = \frac{D_e}{f_{cc} + rK_d} \quad (4)$$

Radioactive decay is neglected here.

3.2 Model domain and spatial discretization

Although radionuclide migration around the repository is fully three dimensional (Genty et al., 2009), radionuclide diffusion exhibits symmetry with respect to the mean horizontal plane of the repository because the repository is located at the middle depth of the Callovo-Oxfordian formation (Figure 2). Therefore, radionuclide migration can be studied in a half of the domain.

Radionuclide migration is assumed to be symmetric with respect to two sets of vertical planes. The first set of symmetry planes contain the axis the disposal cells. The second set of vertical planes pass through the middle point between two adjacent disposal cells. The distance between two adjacent vertical planes of symmetry is equal to the half distance between two adjacent cells which is 6.5 m (Andra, 2005b). For a homogeneous formation, radionuclide migration can be studied in a 2D model domain of $65 \cdot 6.5$ m^2 (see Figure 2). The domain is discretized with a finite element mesh of 4550 triangular elements and 2388 nodes. The size of the elements is small near the disposal cell and increases away from the cell (Figure 3).

There are several stages in the time evolution of radionuclide migration from the disposal cell to the outflow boundary through the C-Ox clay formation. Radionuclides diffuse from the disposal cell into the C-Ox clay in the first stage in an axisymmetric pattern. This stage lasts for a time t^* such that $0 < t < t^*$, where t^* is the time needed for the radionuclide to arrive at the middle point between two adjacent cells. Axial symmetry vanishes in the second stage when the radionuclides migrate both in the horizontal and the vertical directions. The third stage takes place at late times when radionuclide migration is mostly vertical and can be approximated with a 1D vertical grid. Figure 4 shows the contour plots of computed concentrations of HTO and illustrates the three stages.

The origin of Cartesian coordinate system (x,y) is taken at the center of the disposal cell. The model domain is bounded in the horizontal direction at x = 6.5 m and in the vertical direction at y = 65 m, the vertical distance from the cell to the overlying Oxfordian formation. Radionuclide diffusion during the first stage can be studied with a 1D axisymmetric model around disposal cells. The domain is bounded in the horizontal direction at x = 6.5 m.

1D axisymmetric models sometimes are solved by using 1D parallel grids due to code limitations. Computed results with 1D axisymmetric and a 1D parallel grids have been compared to evaluate the errors committed by adopting a 1D parallel grid for solving a 1D axisymmetric problem. The diffusive area in a 1D axisymmetric model depends on the square of the radial distance, *r*, while the diffusive area is constant for a 1D parallel model (see Figure 5). There are several options to set the equivalent thickness of the 1D parallel model, *b*. It can be taken equal to the length of the circumference of the disposal cell, L_i, which is equal to $2\pi R_i$ with R_i = 0.35 m. On the other hand, it can be taken equal to $2\pi R_e$, the length of the circumference corresponding to the half-distance between two adjacent cells, L_e, which is given by $2\pi R_e$ with R_e = 6.5 m. The 1D parallel grid has the same water volume as the 1D axisymmetric grid when the thickness b is equal to the average of L_i and L_e, that is $b = \pi (R_e + R_i)$.

The 1D vertical model of the third stage extends from y = 0 to y = 65 m. In this case, radionuclides are released at y = 0.

3.3 Material zones and boundary conditions

The numerical model considers two material zones: (1) The disposal cell where radionuclides are released and (2) The C-Ox clay formation. The diffusion coefficient for the cell is taken sufficiently large to ensure a homogenous radionuclide concentration within the disposal cell.

The Callovo-Oxfordian formation shows a horizontal stratification with an anisotropic effective diffusion tensor. The horizontal component $D_{e//}$ is 1.56 larger than the vertical component $D_{e\perp}$ (Dewonck, 2007 and Samper et al. 2008b). Transport parameters in the C-Ox clay are radionuclide dependent. The values of the effective diffusion coefficient perpendicular to the stratification, $D_{e-|}$, the accessible porosity, Φ_{cc} and the distribution coefficient, K_d, for HTO, Cl^- and Cs^+ were taken from Dewonck (2007) and were obtained

from laboratory experiments. On the other hand, the transport parameters of $^{238}U(IV)$ were taken from Vahlund et al. (2006). The diffusion and sorption parameters of the radionuclides are listed in Table 1.

The effective diffusion coefficient D_e is taken equal to the horizontal component of the tensor, $D_{e//}$, for 1D transport perpendicular to the axes of the disposal cells while for the 1D vertical model, D_e is taken equal to $D_{e\perp}$.

Background radionuclide concentrations in the clay are assumed equal to zero. Radionuclides are released into the pore space of the disposal cell. Two types of boundary conditions are considered at the disposal cell: a constant concentration and an instantaneous unit pulse. These boundary conditions are imposed at the nodes lying in the disposal cell. The unit mass of the tracer is added instantaneously to the volume of water contained in the disposal cell. Similar to Samper et al. (2009b), it is assumed that disposal cells may contain 100 L of water per meter of cell. The rest of the external boundaries are impervious except for the top outflow boundary at the contact with the Oxfordian limestone where the concentration is prescribed to zero.

Model results are presented in terms of relative concentrations which are normalized by either the boundary or the initial concentrations.

3.4 Computer code

Radionuclide migration has been modeled with CORE^{2D} V4, a general-purose non-isothermal multicomponent reactive transport code for two-dimensional saturated/unsaturated porous and fractured media (Samper et al. 2003; 2009a; 2011). It can solve simultaneously for groundwater flow, heat transport and multi-component reactive solute transport in saturated or unsaturated steady state or transient groundwater flow under general boundary conditions. CORE^{2D} has been widely used to model laboratory and *in situ* experiments performed for HLW disposal (Molinero and Samper 2006; Samper et al., 2008c; Zheng and Samper, 2008; Zheng et al., 2008, 2010), evaluate the long-term geochemical evolution of radioactive waste repositories in clay (Yang *et al.,* 2008), model the transport of corrosion products and their geochemical interactions with bentonite (Samper et al., 2008a) and evaluate the long-term transport and sorption of radionuclides through

the bentonite barrier (Samper et al., 2010). The model results presented here use only the most basic features of CORE^{2D}. Its most advanced features will be used in the next stages of the study.

4. Model results

4.1. 2D model results

Figure 4 shows the contour plots of computed concentrations of HTO at 10^3, 10^4, 10^5 and 10^6 years for a constant concentration at the disposal cell. Contour lines are axisymmetric for $t < 10^3$ years. In the second stage when HTO reaches the bottom right boundary at (6.5, 0), contour lines are no longer symmetric. The asymmetry of the migration can be observed clearly in the contour plots corresponding at $t = 10^4$ and 10^5 years. Contour plots become nearly horizontal and the diffusive flux is approximately vertical for $t > 10^5$ years.

Diffusion patterns are different for each radionuclide because the diffusive rate is proportional to the apparent diffusion coefficient. The diffusive rate of $^{238}U(IV)$ is two orders of magnitude slower than that of $^{133}Cs^+$ which in turn is two orders of magnitude slower than those of HTO and $^{36}Cl^-$ (see Table 1). The contour line corresponding to a relative concentration of 0.1 for HTO after $t = 10^3$ years is located at a distance of 3.2 m from the disposal cell. Such distance is 2.7 m for $^{36}Cl^-$. For $^{133}Cs^+$ it is 0.7 m while for $^{238}U(IV)$ is two orders of magnitude smaller than that of HTO (see Figure 6). Furthermore, diffusion shows axial symmetry until $t = 10^4$ years for $^{133}Cs^+$ and $t = 10^6$ years for $^{238}U(IV)$.

Diffusion patterns are also different depending on the boundary condition at the disposal cell. The radionuclide mass released at the disposal cell with an instantaneous pulse is smaller than the mass injected with a constant concentration. Therefore, concentration gradients with an instantaneous pulse dissipate faster than in the case of constant concentration.

4.2 1D axisymmetric models

Radionuclide migration through the C-Ox clay formation has been simulated by using two 1D axisymmetric models around the disposal cell. They differ in the position of the outer boundary. The first model is the so-called bounded model in which the outer boundary is located at r = 6.5 m to account for the

boundary effect of two adjacent cells. The second model is denoted here as the "unbounded model". It disregards the effect of the neighbor cell. The outer boundary of this model is located at a distance of 65 m to account for the effect of the top boundary. The results of both models are identical as long as the radionuclides do not reach the location at r = 6.5 m. Later, the radionuclide concentrations for the bounded model at that location are larger than those computed with the unbounded model due to the boundary effect.

The arrival time of a radionuclide to r = 6.5 m is the time needed for the relative concentration of the radionuclide to attain a threshold value greater than zero. Arrival times have been computed for threshold concentrations of 10^{-3} and 10^{-6} (see Table 2). A bounded model is acceptable for $^{238}U(IV)$. It is only acceptable for $t < 8 \cdot 10^3$ years for $^{133}Cs^+$ for a constant concentration and $t < 2.3 \cdot 10^4$ years for an instantaneous pulse. It is acceptable only for t < 120 years for HTO and $^{36}Cl^-$.

4.3 1D parallel and axisymmetric models

Model results computed with a 1D parallel model for several values of the thickness b are compared to those calculated with the 1D axisymmetric model. Figure 7a shows the comparison of the breakthrough curves at r = 6.5 m for HTO and $^{133}Cs^+$ calculated with the 1D radial and parallel models for a constant concentration at the cell. The results of the 1D parallel model in this case do not depend on the value of b. The concentrations computed with both models are markedly different for all the radionuclides. The 1D parallel model predicts a faster arrival of the radionuclides at the boundary than the 1D axisymmetric model.

In the case of an instantaneous mass pulse, M, the computed concentrations varies with b because the solution depends on the mass per unit thickness, M/b, which decreases when b increases. Therefore, computed concentrations are largest for the minimum b (Figure 7.b). The comparison of computed HTO concentrations at the disposal cell and at the external boundary (r = 6.5 m) for several values of b show that the differences between the results of the 1D parallel and 1D axisymmetric models increase with time and are largest for the minimum b (see Figure 7b and 7c). The results of the 1D parallel model for HTO are very inaccurate for the minimum and the maximum values of b. Computed results coincide with those of the 1D axisymmetric after 2000 years for the average value of b. The conclusions for $^{36}Cl^-$ are similar to those of HTO. For $^{133}Cs^+$ and

^{238}U(IV), however, the 1D parallel model deviates significantly from the 1D axisymmetric model regardless the value of b (not shown here).

4.4. Comparison of the 2D and the 1D vertical models

The 1D parallel model in the vertical direction assumes that the radionuclide mass, M, is released instantaneously and uniformly throughout the bottom boundary at z = 0 corresponding to the depth of the disposal cells. The 1D vertical model neglects the horizontal component of the diffusive flux which is especially relevant at intermediate times. Figure 8 shows the comparison of the computed concentrations with the 2D and the 1D vertical models along the vertical line passing through the disposal cell. In the case of a constant concentration at the disposal cell, the concentrations of all radionuclides computed with the 1D vertical model deviate largely from those computed with the 2D model. The results of the 1D vertical model agree with those of the 2D model only after 10^4 years and for conservative radionuclides released instantaneously (Figure 8).

5. Conclusions

Conceptual and numerical models of radionuclide diffusion and sorption around a radioactive waste repository in clay according to the French reference concept have been presented for HTO, $^{36}Cl^-$, $^{133}Cs^+$ and ^{238}U (IV). Radionuclides are released into the disposal cell either at a fixed concentration or as an instantaneous unit pulse. Models of increasing dimensionality have been performed for: 1) 1D transport perpendicular to the axes of the disposal cells; 2) 1D axisymmetric transport around disposal cells for bounded and unbounded domains; 3) 2D transport through vertical planes; and 4) 1D vertical transport from the disposal cells into the overlying Oxfordian formation. The results of the 1D unbounded model are always acceptable for ^{238}U. Such model is valid for $^{133}Cs^+$ for $0 < t < 10^4$ years while it is valid for HTO and $^{36}Cl^-$ only for $t < 10^3$ years. Computed concentrations with the 1D parallel and the 1D axisymmetric models are markedly and, therefore, the use of the 1D parallel model for the long-term modeling of radionuclide migration from the repository should be avoided. The 1D vertical model is valid only for conservative radionuclides released instantaneously and leads always to large errors for all radionuclides for a constant concentration.

Here we have presented the results of the first step of our study for the selection of the most appropriate assumptions and simplifications for the numerical model of the geochemical evolution and radionuclide migration in a radioactive waste repository. The next steps will account for: 1) The decay of radionuclides; 2) The time evolution of the geochemical conditions using reactive transport models; 3) The spatial variability of clay parameters; 4) The uncertainties in the boundary conditions of the CO-x clay formation and the porosity of the disposal cells; and 5) The actual 3D configuration of the repository.

6. Acknowledgements

This work was supported by the European Union through the PAMINA Project ((FP6-036404), the University of A Coruña through a research scholarship awarded to the third author, the Spanish Ministry of Science and Technology through project CGL2006-09080 and a research scholarship awarded to the second author, the Xunta de Galicia (Maria Barbeito Program) through a research scholarship awarded to the fourth author. Parts of this work were performed during the sabbatical stay of Javier Samper at the University of Strasbourg from October 2008 to August 2009 which was supported by the University of A Coruña, the Spanish Ministry of Science and Technology and the University of Strasbourg. We thank also E. Ledoux and Angelo Borrelli for their comments and recommendations which have improved the paper.

7. References

Andra (2005a). *Dossier 2005 Argile –Synthèse: Evaluation de la faisabilité du stockage géologique en formation argileuse.*

Andra (2005b). *Dossier Argile –Tome: Arquitecture et gestion du stockage géologique.*

Bear, J. (1978) Dynamics of fluids in porous media. Dover, NY, USA

Dewonck, S. (2007) *Experimentation DIR: Synthèse des résultats obtenus au 01/03/07.* Rapport Andra D.RP.ALS.07.0044.

Duro, L., Grivé, M., Cera E, Gaona X, Domènech C, Bruno, J., (2006). Determination and assessment of the concentration limits to be used in SR-Can. SKB Technical report TR-06-32.

Genty A, G. Mathieu & E Weetjens (2009) Benchmark calculations in clay, Deliverable 4.2.4 of PAMINA Integrated Project.

Khan, S.A. (2003). Sorption of the long-lived radionuclides cesium-134, strotium-85 and cobalt-60 on bentonite. Journal of Radioanalytical and Nuclear Chemistry 258 (1), 3-6.

Molinero, J., Samper, J., (2006). Modeling of reactive solute transport in fracture zones of granitic bedrocks. J. Cont. Hydrol., 82, 293–318.

Montavon, G., Alhajji, E. And Grambow, B. (2006). Study of the interaction of Ni^{2+} and Cs^{+} on MX-80 bentonite: effect of compaction using the "Capillary method". Environmental Science and Technology 40, 4672-4679.

Murali, M.S. and Mathur, J.N. (2002). Sorption characteristics of Am(III), Sr(II) and Cs(I) on bentonite and granite. Journal of Radioanalytical and Nuclear Chemistry 254(1), 129-136.

Lu, C, J Samper, B. Fritz, A. Clement & L. Montenegro (2011) Interactions of corrosion products and bentonite: An Extended multicomponent reactive transport model, Physics and Chemistry of the Earth (accepted).

Marty, N., Fritz, B., Clément, A., Michau, N. (2010). *Modeling the long term alteration of the engineered bentonite barrier in an underground radioactive waste repository.* Applied Clay Sci. 47, 1-2, 82-90.

Mathieu, G., Pellegrini, D., Serres, C., (2006). *Modeling of cement/clay interactions, gas transport and radionuclide transport*. D5.1.9. NF-PRO Project, European Commission.

Omel'yanenko, B.I., Petrov, V.A., Poluektov, V.V. (2007). Behavior of uranium under conditions of interaction of rocks and ores with subsurface water. Geology of Ore Deposits, Vol. 49, No. 5, pp. 378-391.

Pepin, G, F Plas, K.F. Nilsson, & S Prvakova (2008) Second Benchmark specification for the uncertainty analysis based on the example of the French clay site, Milestone M 4.3.3 of PAMINA Integrated Project.

Samper, J., Yang, C., Montenegro, L. (2003) Users manual of CORE2D version 4: A COde for groundwater flow and REactive solute transport. Universidad de A Coruña, A Coruña, Spain.

Samper, J., Yang, Ch., Montenegro, L., Bonilla, M., Lu, C., Yang, Q., Zheng, L. (2007) *Mass and energy balance and flux calculations for radionuclide release and geochemical evolution for SF carbon steel HLW repositories in clay and granite.* D5.1.13. NF-PRO Project, European Commission.

Samper, J., Lu, C., Montenegro, L. (2008a) Coupled hydrogeochemical calculations of the interactions of corrosion products and bentonite, Physics and Chemistry of the Earth, Vol. 33, Supplement 1, S306-S316.

Samper, J., Q. Yang, S. Yi, M. García-Gutiérrez, T. Missana, M. Mingarro, Ú. Alonso, J.L. Cormenzana, (2008b) *Numerical modelling of large-scale solid-source diffusion experiment in Callovo-Oxfordian clay,* Physics and Chemistry of the Earth, Vol. 33. Supplement 1, S208-S215 doi:10.1016/j.pce.2008.10.011.

Samper J., L. Zheng, A.M. Fernández and L. Montenegro (2008c) Inverse modeling of multicomponent reactive transport through single and dual porosity media, J. Cont. Hydrol., Vol 98/3-4 pp 115-127.

Samper, J., Xu, T., Yang, C. (2009a). *A sequential partly iterative approach for multicomponent reactive transport with CORE^{2D}.* Computer Geoscience DOI 10.1007/s10596-008-9119-5.

Samper, J., Lu, C., Cormenzana, J.L., Ma, H., Cuñado, M.A., (2009b), Benchmark calculations in granite, Deliverable 4.1.2 of PAMINA Integrated Project.

Samper J, C Lu, JL Cormenzana, H Ma, L Montenegro & MA Cuñado (2010) Testing K_d models of Cs^+ in the near field of a HLW repository in granite with a reactive transport model, Physics and Chemistry of the Earth, Vol 35:278–283 doi:10.1016/j.pce.2010.04.002.

Samper, J., Yang, C., Zheng, L., Montenegro, L., Moreira, S., Lu, C. (2011). *CORE^{2D} V4: A code for water flow, heat and solute transport, geochemical reactions, and microbial processes.* Electronic book on Reactive Transport Modelling. Chapter 7.

Vahlund F.J., Andersson, J.A., Streamflow AB, Löfgren, M. (2006*). Data report for the safety assessment. SR-Can*. SKB Technical Report TR-06-25.

Yang, C., J. Samper, & L. Montenegro (2008) A coupled non-isothermal reactive transport model for long-term geochemical evolution of a HLW repository in clay, Environmental Geology, 53, 1627–1638. DOI 10.1007/s00254-007-0770-2.

Zheng, L. and J. Samper (2008) Coupled THMC model of FEBEX mock-up test, Physics and Chemistry of the Earth, Physics and Chemistry of the Earth, Vol. 33, S486–S498. doi:10.1016/j.pce.2008.10.023.

Zheng, L., J. Samper, L. Montenegro & J.C. Mayor (2008) Flow and reactive transport model of a ventilation experiment in Opallinus clay, Physics and Chemistry of the Earth, Vol. 33. Issues 14-16, 1009-1018. doi:10.1016/j.pce.2008.05.012

Zheng L, J Samper, L Montenegro, AM Fernández (2010) A coupled THMC model of a heating and hydration laboratory experiment in unsaturated compacted FEBEX bentonite, Journal of Hydrology. 10.1016/j.jhydrol.2010.03.009 .

Table 1. Radionuclide diffusion and sorption parameters in clay: $D_{e\perp}$ and $D_{e//}$ are the vertical and horizontal effective diffusion components, Φ_{cc} is the accessible porosity, K_d is the distribution coefficient, and $D_{a//}$ is the horizontal component of the apparent diffusion.

Radionuclide	$D_{e\perp}$ (m^2/s)	$D_{e//}$ (m^2/s)	Φ_{cc}	K_d (L/Kg)	$D_{a//}$ (m^2/s)
HTO	$2.6\cdot10^{-11}$	$4.1\cdot10^{-11}$	0.18	0	$2.2\cdot10^{-10}$
$^{36}Cl^-$	$6.2\cdot10^{-12}$	$9.7\cdot10^{-12}$	0.06	0	$1.6\cdot10^{-10}$
$^{133}Cs^+$	$2.3\cdot10^{-10}$	$3.6\cdot10^{-10}$	0.18	50	$3.3\cdot10^{-12}$
$^{238}U(IV)$	$1.2\cdot10^{-10}$	$1.9\cdot10^{-10}$	0.18	3000	$2.9\cdot10^{-14}$

Table 2. Arrival times of the radionuclides to the boundary located at the plane of symmetry located at the middle point between two adjacent cells. Results are listed for two threshold relative concentrations $\mathbf{C/C_o}$ and two types of boundary conditions at the disposal cell: constant concentration and instantaneous pulse. Here * means that the radionuclide does not reach this point for the simulation time of 1Ma.

Radionuclide	Arrival times (years)			
	Constant concentration		Instantaneous pulse	
	$C/C_o > 10^{-6}$	$C/C_o > 10^{-3}$	$C/C_o > 10^{-6}$	$C/C_o > 10^{-3}$
HTO	112	273	122	437
$^{36}Cl^-$	157	381	162	463
$^{133}Cs^+$	7648	18650	22930	*
$^{238}U(IV)$	881600	*	*	*

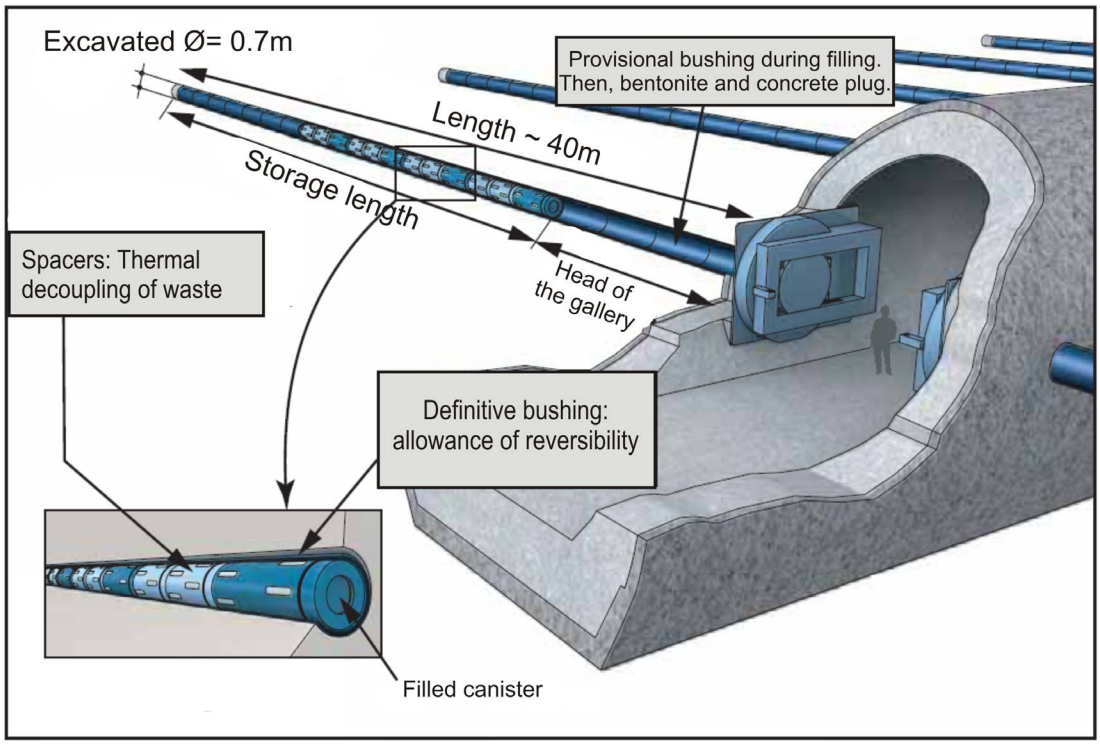

Figure 1. Setup of the repository for wastes type C (modified from ANDRA, 2005a).

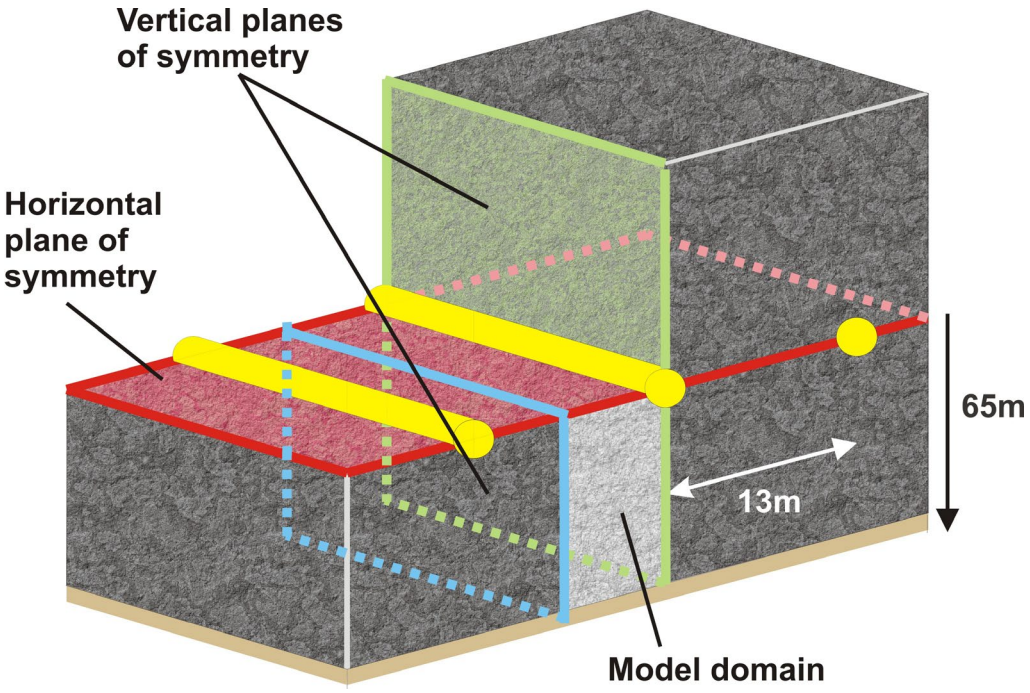

Figure 2. Sketch of the disposal cells layout in the C-Ox clay formation showing the 2D model domain and the following three planes of symmetry: 1) A horizontal plane which divides the cells in two equal parts; 2) A vertical plane that divides the cells vertically in two parts and 3) A vertical plane equidistant to two adjacent cells.

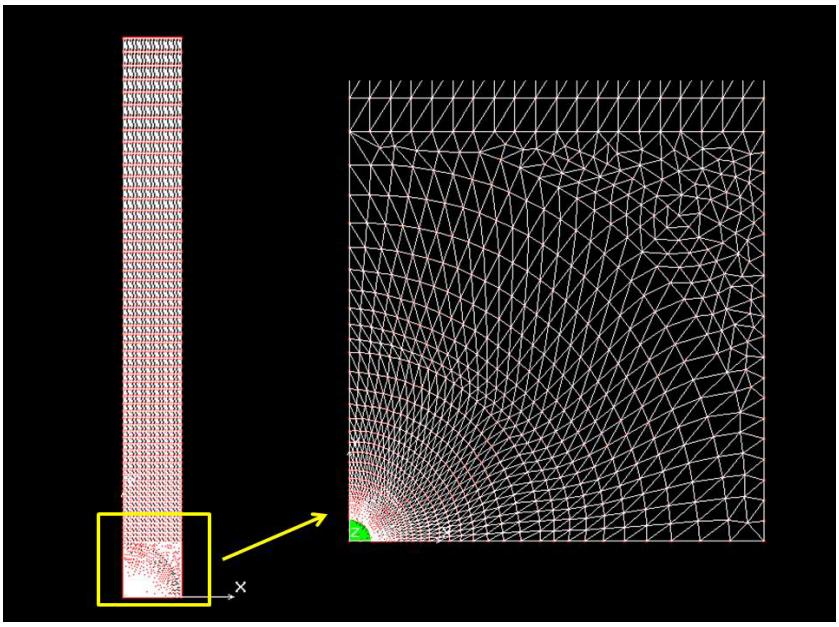

Figure 3. Finite elements mesh of the 2D model which extends over a domain of 6.5·65 m^2. Also shown is a zoom of the area around the disposal cell.

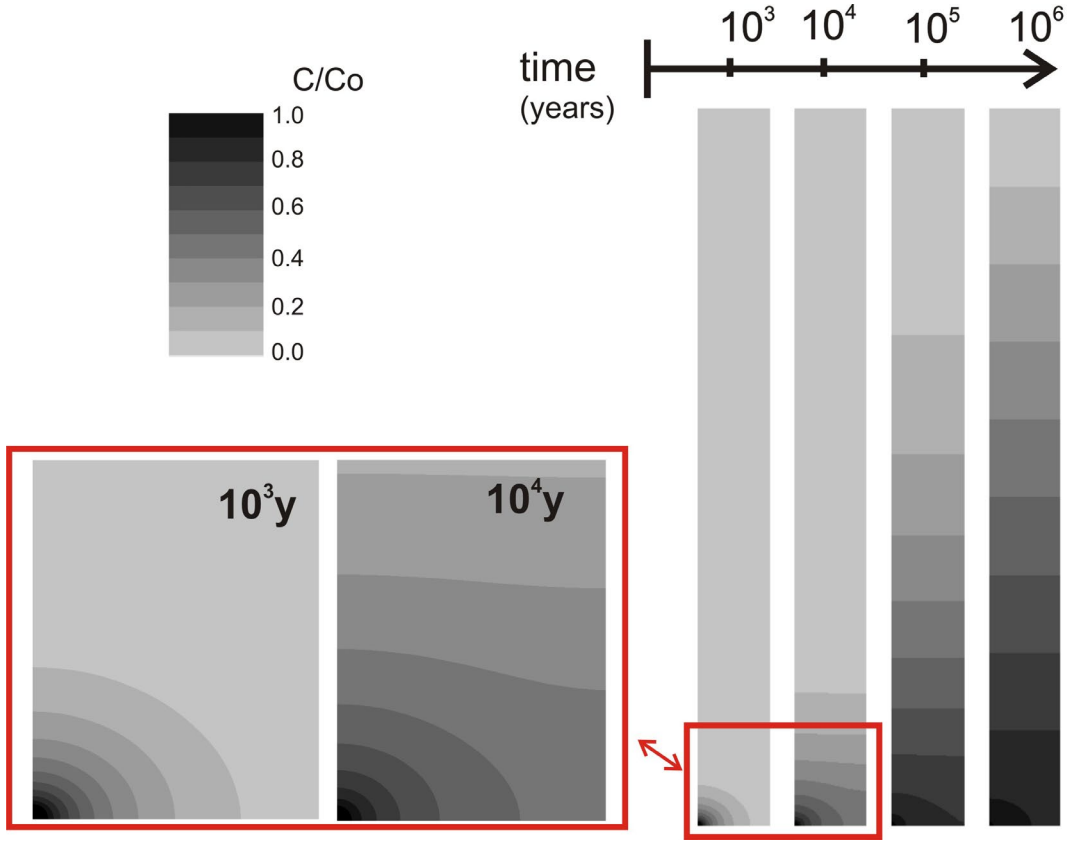

Figure 4. Computed HTO concentrations with a 2D model at 10^3, 10^4, 10^5 and 10^6 years. HTO transport is axisymmetric for $t < 10^3$ years. Transport is 2D for $10^4 < t < 10^5$ years. The diffusive flux at late times is approximately 1D vertical.

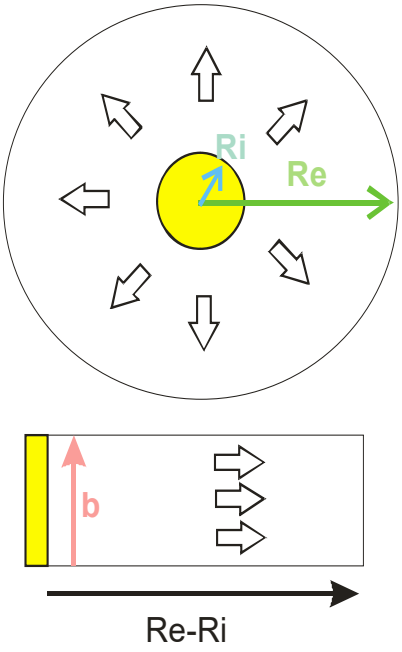

Figure 5. Sketch of the 1D axysymmetric and 1D parallel models. R_i and R_e are the internal and external radii.

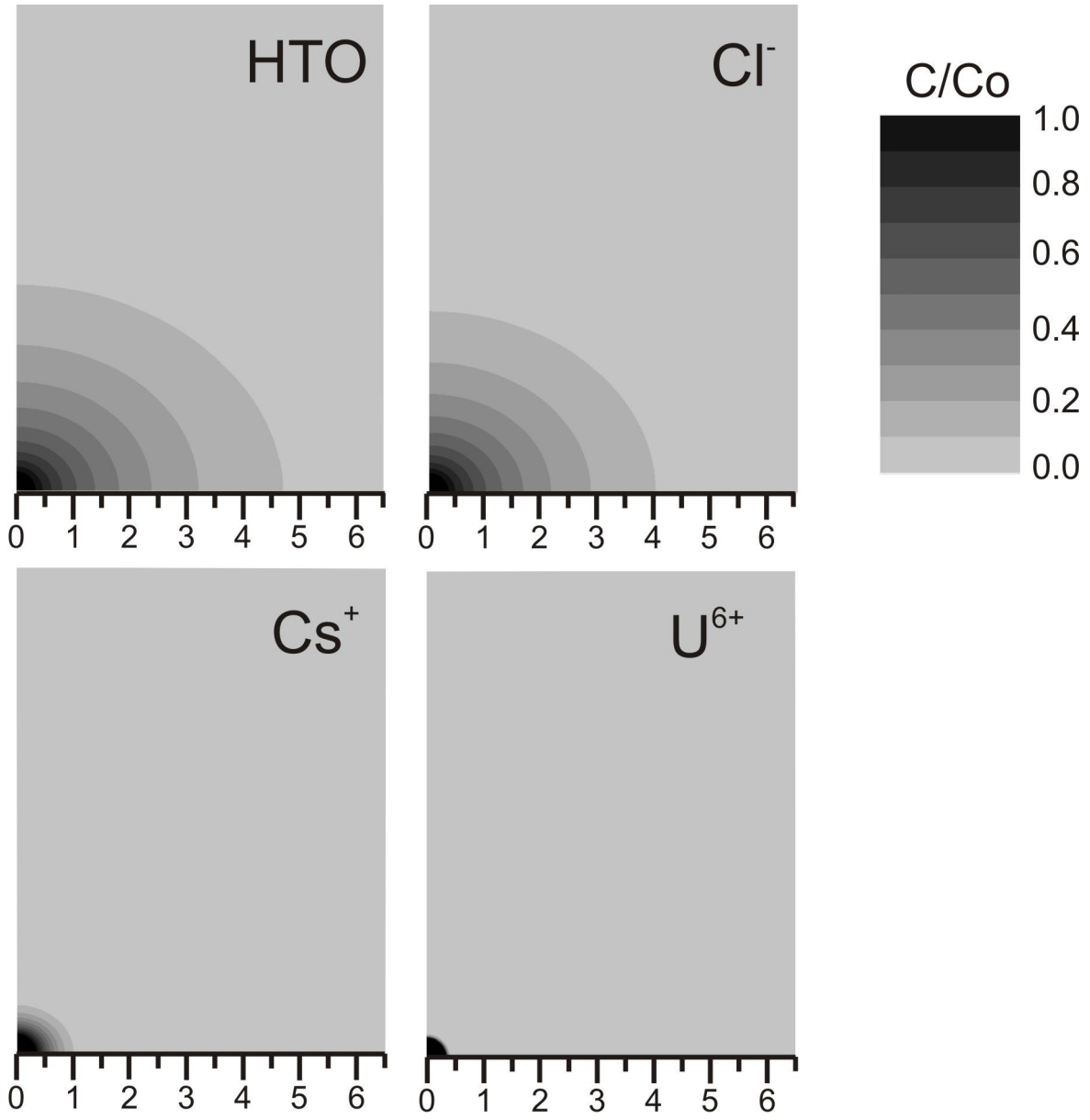

Figure 6. Computed radionuclide concentrations with a 2D model at 10^3 years considering a constant radionuclide concentration at the disposal cell. Transport is axisymmetric for all the tracers at this time. The relative concentration is larger than 0.1 for distances to the disposal cell smaller than 3.2 m for HTO, 2.7 m for $^{36}Cl^-$, 0.7 m for $^{133}Cs^+$ and 0.4 m for $^{238}U(IV)$.

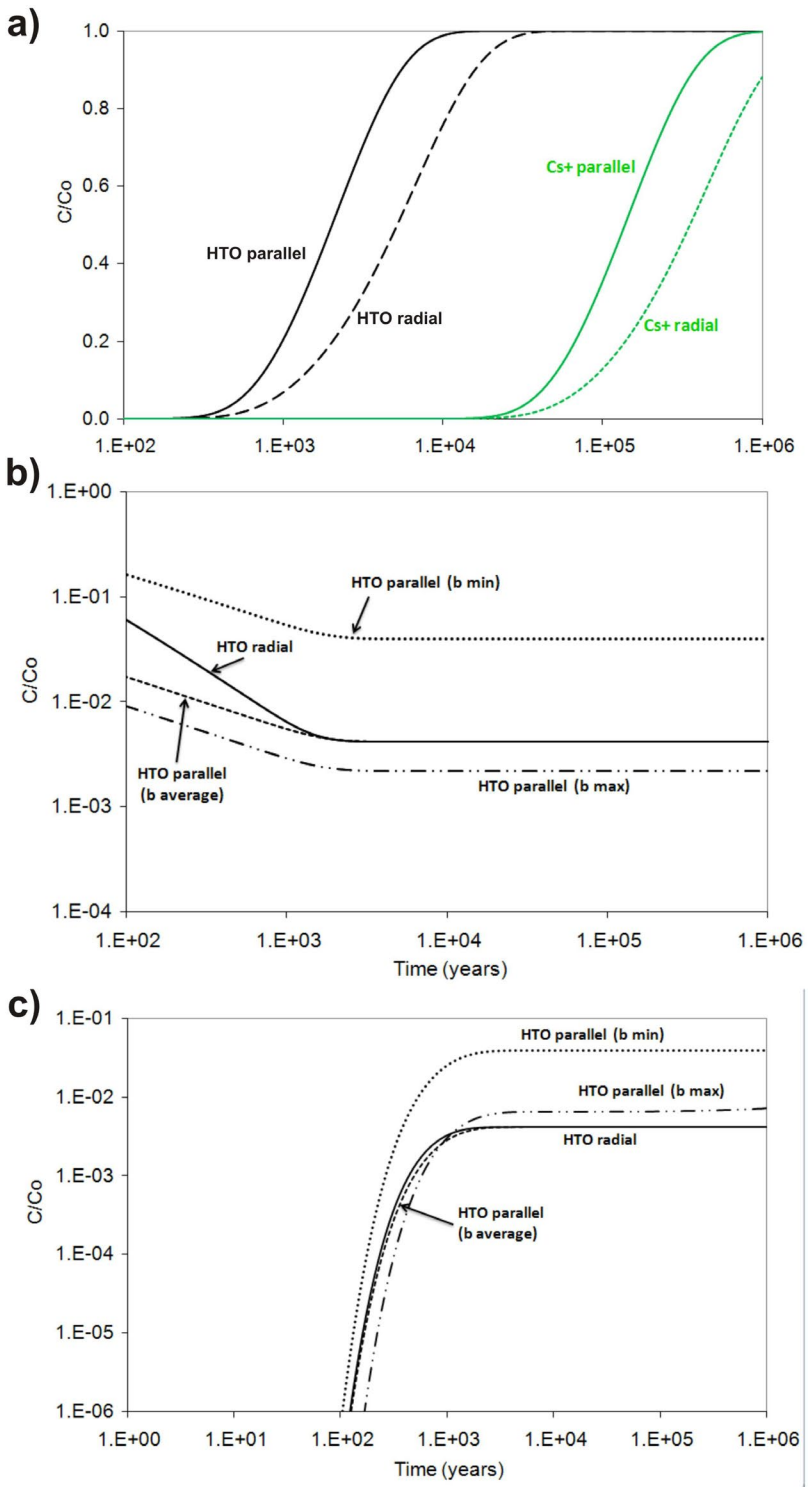

Figure 7. Comparison of the computed concentrations using the 1D axysymmetric and 1D parallel models: (a) Comparison of HTO and $^{133}Cs^{+}$ concentrations at the boundary located 6.5 m from the disposal cell axis for the case of constant concentration at the disposal cell. (b) Comparison of HTO dilution at the disposal cell in the case of an instantaneous pulse for different values of b. (c) Comparison of HTO computed concentrations at the boundary (r = 6.5 m) in the case of an instantaneous pulse for different values of b.

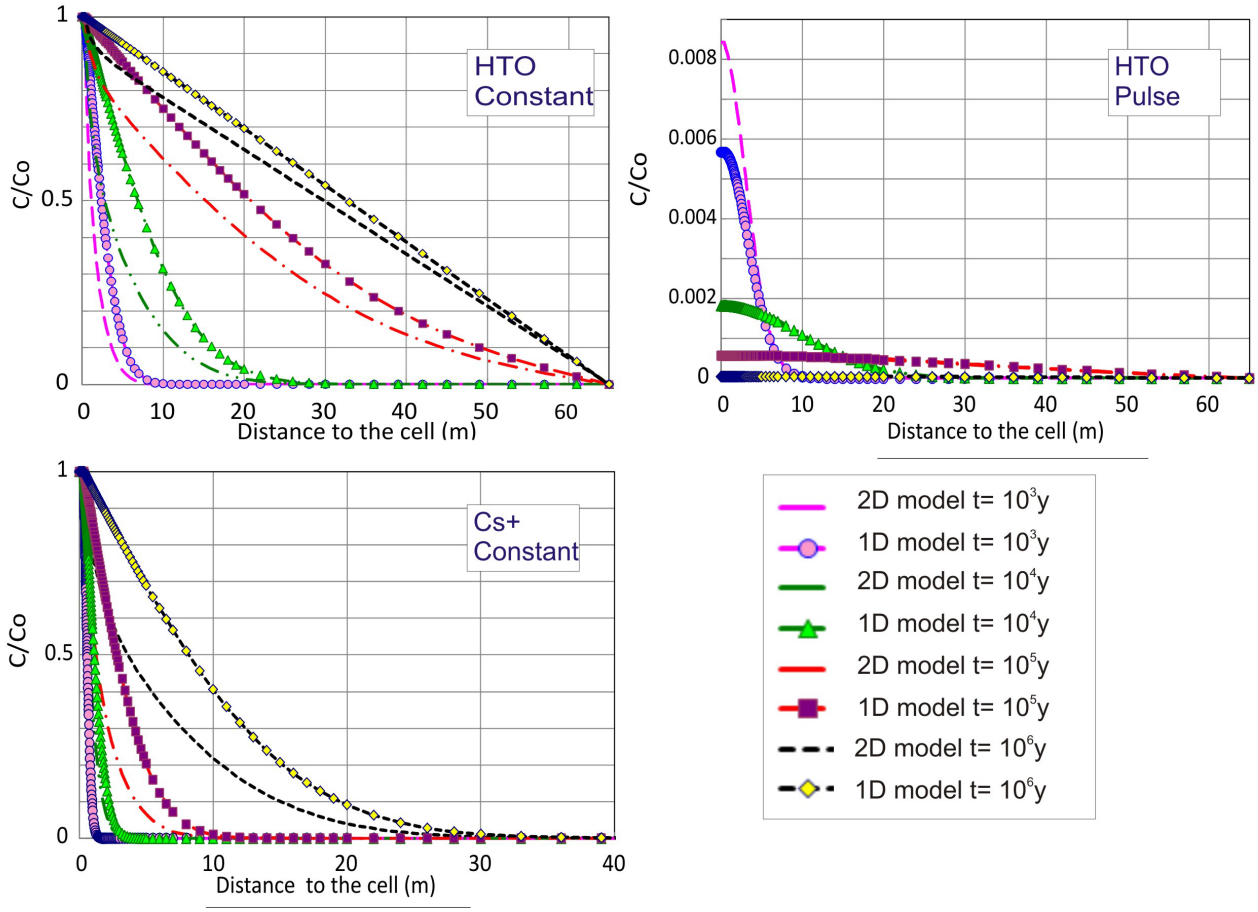

Figure 8. Comparison of the concentration profiles along the left boundary computed with the 2D and the 1D vertical models. Results are presented for HTO considering a constant concentration (top left) and an instantaneous pulse (top right) and for $^{133}Cs^{+}$ (bottom) considering a constant concentration at the cell.